コンピュータビジョンと
イメージメディア 137－20
（２００３．３．２８）

多視点パノラマ映像の数理

鳥居 秋彦† 井宮 淳††

† 千葉大学 自然科学研究科 〒263-8522 千葉稲毛区弥生町 1-33 Tel +81-43-290-3257.
†† 国立情報学研究所 / 総合研究大学院大学 / 千葉大学総合メディア基盤センター
〒101-8430 東京都千代田区一ツ橋 2-1-2 // 〒263-8522 千葉稲毛区弥生町 1-33
Tel +81-3-4212-2000 // +81-43-290-3257
†,†† {akit,imiya}@media.imit.chiba-u.ac.jp

あらまし 本論文は，全方位カメラシステムとパノラマカメラシステムで成立する多視点幾何学を定式化する．多視点パノラマカメラの幾何，代数拘束条件が，その定式化から導かれる．さらに，その拘束条件に従うことで，広範囲領域に渡り存在する３次元物体の復元を可能にする．

キーワード 多視点幾何学，全方位カメラ，パノラマカメラモデル，線カメラモデル，３次元物体復元．

Mathematics of a Multiple-Panorama-Camera System

Akihiko TORII† and Atsushi IMIYA††

†School of Science and Technology, Chiba University Yayoicho 1-33, Inage-ku, 263-8522, Chiba, Japan Tel +81-43-290-3257.
††National Institute of Informatics / Department of Informatics, the Graduate University for Advanced Studies / IMIT, Chiba University Hitotsubashi 2-1-2, Chiyoda-ku, 101-8430, Tokyo, Japan // Yayoi-cho 1-33, Inage-ku, 263-8522, Chiba, Japan
Tel ++81-3-4212-2000 // +81-43-290-3257.
†,†† {akit,imiya}@media.imit.chiba-u.ac.jp

Abstract We formulate multiple-view geometry for omni-directional and panorama-camera systems. The mathematical formulations enable us to derive the geometrical and algebraic constraints for multiple panorama-camera configurations. The constraints permit us to reconstruct three-dimensional objects for a large feasible region.

Key Words Multiple-View Geometry, Omni-Directional Cameras, Panorama Cameras, Line Cameras, Reconstrucsion

1 Introduction

In this paper, we formulate multiple-view geometry for omni-directional and panorama-camera systems. The mathematical formulations enable us to define the geometrical and algebraic constraints for multiple panorama-camera configurations. The configurations derive a larger feasible region for the three-dimensional reconstruction of objects than usual omni-directional and panorama-camera systems.

Multiple-view geometry for pin-hole cameras studied in the computer vision community. The well-known algebraic constraints for the multiple-view geometry were introduced, such as epipolar constraints equivalently bilinear form [1], [2] for stereo views, the trifocal tensor [2], [3] for three views, the quadrifocal tensor [4], [5] for four views and the factorization method [6] for multiple views. On the other hand, T. Svoboda, T. Pajdla and V. Hlavac introduced the geometrical constraint for stereo systems of omni-directional cameras [7]. However, three or more view geometrical constraints are not clearly represented for the omni-directional cameras. Our aim in this study is to derive the geometrical and algebraic constraints for multiple omni-directional cameras.

Recently, T. Sugimura and J. Sato proved [8] that the number of algebraic constraints in the trifocal tensor is reduced if cameras mutually image their epipoles. This geometrical condition restricts the geometrical configuration of pin-hole cameras, because multiple pin-hole camera systems can not always observe the epipoles of their cameras. Here, we assume omni-directional cameras are located parallel on the same plane. These omni-directional camera systems satisfy the geometrical condition that they always observe the epipoles of their cameras, because the omni-directional camera always images the other cameras. Therefore, Sato's condition could be achieved with multiple omni-directional camera systems.

In this paper, we analyze the geometrical configurations of omni-directional camera systems fulfilling the conditions for the multiple-view geometry to reduce the number of constrains for the multiple camera systems. This is the first step to establish the multiple-view geometry for omni-directional camera systems as a generation from multiple-view geometry for pin-hole camera systems to multiple-view geometry for omni-directional camera systems.

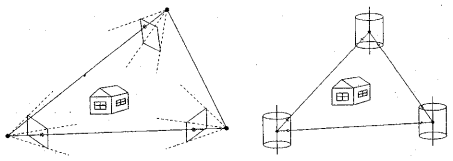

(a) (b)

Figure 1: Geometrical configurations of a pin-hole camera system and an omni-directional camera system to image epipoles mutually.

2 Panoramic Image

A sequence of pin-hole camera images enables us to synthesize a wide view image comparing to the image observed by a camera. The synthesized image from a sequence of images is generally called a panoramic image. Since a point and a line are fundamental elements for imaging, many camera models could be geometrically constructed from the two essential elements for imaging. Therefore, we formulate a camera model with lines and points for our applications.

2.1 Line-Camera Model

Definition 1 *A line camera is a collection of rays which pass through a single point on a plane in a space. A line-camera model consists of a line-camera center which is the single point, an image line and a camera axis which intersects the line-camera center and is parallel to the image line.*

We assume that the line-camera center $\boldsymbol{C} = (0,0,0)^\top$ is located at the origin of the world coordinate system. For the line camera axis $\boldsymbol{r}_c$, we set $\boldsymbol{r}_c = k(0,0,1)^\top$ for $k \in \mathbf{R}$, that is, the direction of $\boldsymbol{r}_c$ is the direction of the z axis. For the image line $\boldsymbol{l}$ of the line camera on the x-z plane ($y = 0$), a point $\boldsymbol{X} = (X,0,Z)^\top$ in a space is projected to the point $\boldsymbol{x} = (x,0)^\top$ on the image line $\boldsymbol{l}$ according to the formulation

$$x = f\frac{X}{Z}, \tag{1}$$

where f is the focal length of the line camera.

2.2 Line-Motion Camera Model

The motion of a line camera along the direction of the y axis yields a collection of image lines $\{\boldsymbol{l}_t\}_{t=1}^n$

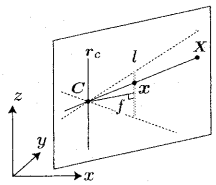

Figure 2: A line-camera model.

as illustrated in figure 3 (a) and (b). In figure 3 (c), d_t is the distance between the lines $\boldsymbol{l}_t$ and $\boldsymbol{l}_{t+1}$. If we set $d_t \to 0$, the collection of the image lines $\{\boldsymbol{l}_t\}_{t=1}^n$ forms a rectangular image plane. Assuming the collection of parallel imaging lines as a single camera model, such a camera model has the same geometrical property with a normal camera with respect to the y direction.

Definition 2 *A line-motion camera is a collection of rays which pass through a single line in a space. A line-motion camera consists of a line-motion camera center which is the single line and a image plane.*

A line-motion camera projects a point $\boldsymbol{X} = (X, Y, Z)^\top$ in a space to the point $\boldsymbol{x} = (x, y)^\top$ on the rectangular image plane according to the equations

$$x = f\frac{X}{Z}, \quad y = Y, \tag{2}$$

where f is the focal length of the line-motion camera.

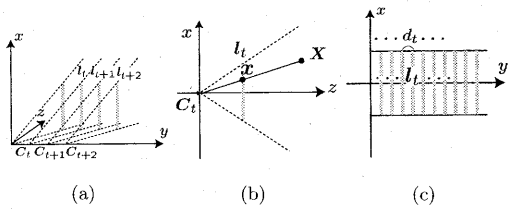

Figure 3: The parallel translation of a line camera constructs a line-motion camera.

2.3 Panorama-Camera Model

The rotation of a line camera around the camera axis $\boldsymbol{r}_c$ yields a collection of image lines $\{\boldsymbol{l}_i\}_{i=1}^n$ and a collection of planes $\{\alpha_i\}_{i=1}^n$ as illustrated in figure 4 (a). The plane α_i includes the image line $\boldsymbol{l}_i$ and the line-camera center $\boldsymbol{C}$. In figure 4 (a), ω_i is the angle between the planes α_i and α_{i+1}. If we set $\omega_i \to 0$ and $\boldsymbol{l}_{n+1} = \boldsymbol{l}_1$, the collection of the parallel image lines $\{\boldsymbol{l}_i\}_{i=1}^n$ forms a cylindrical-image surface. We consider that the collection of these image lines $\{\boldsymbol{l}_i\}_{i=1}^n$ and the camera center $\boldsymbol{C}$ construct a camera model.

Definition 3 *A panorama camera is a collection of rays which pass through a single point in a space. A panorama camera consists of a panorama-camera center which is the single point, a cylindrical-image surface and a camera axis which intersects the panorama-camera center and is parallel to the cylindrical-image surface.*

We assume that the panorama-camera center $\boldsymbol{C}_p = (0, 0, 0)^\top$ is located at the origin of the world coordinate system. For the line camera axis $\boldsymbol{r}_p$, we set $\boldsymbol{r}_p = k(0, 0, 1)^\top$ for $k \in \mathbf{R}$, that is, the direction of $\boldsymbol{r}_p$ is the direction of the z axis. A point $\boldsymbol{X} = (X, Y, Z)^\top$ in a space is projected to the point $\boldsymbol{x}_p = (x_p, y_p, z_p)^\top$ on the cylindrical-image surface according to the formulation

$$\boldsymbol{x}_p = \frac{f}{\sqrt{X^2 + Y^2}}\boldsymbol{X}, \tag{3}$$

where f is a focal length of the panorama camera, as illustrated in figure 4 (b). Here, we transform the cylindrical-image surface to a rectangular panoramic image. We set a point on the rectangular panoramic image is $\boldsymbol{p} = (u_p, v_p)^\top$. The points $\boldsymbol{p}$ and $\boldsymbol{x}$ satisfy the equations

$$u_p = f_s \tan^{-1}\frac{y_p}{x_p}, \quad v_p = f_s \tan^{-1}\frac{z_p}{\sqrt{x_p^2 + y_p^2}}, \tag{4}$$

where f_s is a scale factor for transforming from the cylindrical-image to the rectangular image.

3 Hyperbolic-Camera Model

An omni-directional camera is constructed with a pin-hole camera and a mirror. A hyperbolic camera enables to image the largest region in such omni-directional cameras [9]. We deal with a hyperbolic camera which practically observes an omni-directional image. In figure 5, the focal point of the hyperbolic surface S is $\boldsymbol{F} = (0, 0, 0)^\top$ at the origin of the world coordinate system. The camera center of the hyperbolic camera is $\boldsymbol{C} = (0, 0, -2e)$. The

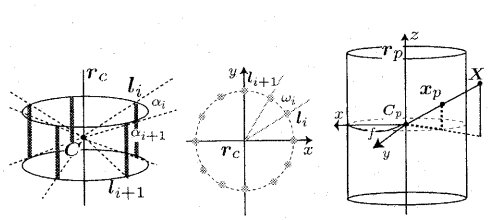

(a) (b)

Figure 4: (a) : The rotation of a line camera constructs a panorama-camera model. We set ω_i is the angle between the planes which pass through the camera center $\boldsymbol{C}$ and the image lines $\boldsymbol{l}_i$ and $\boldsymbol{l}_{i+1}$, respectively. (b) : A panorama-camera model.

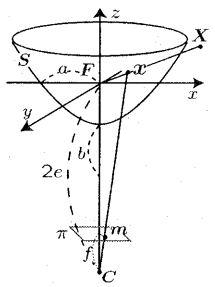

Figure 5: A hyperbolic-camera model. A point $\boldsymbol{X}$ in a space is transformed to the point $\boldsymbol{x}$ on the hyperboloid and $\boldsymbol{x}$ is transformed to the point $\boldsymbol{m}$ on image plane. The geometrical property of reflected ray constructs the camera model with a hyperbolic mirror.

hyperbolic-camera axis r_h is the line which connects $\boldsymbol{C}$ and $\boldsymbol{F}$. We set the hyperbolic surface

$$S : \frac{x^2+y^2}{a^2} - \frac{(z+e)^2}{b^2} = -1, \tag{5}$$

where $e = \sqrt{a^2+b^2}$. A point $\boldsymbol{X} = (X, Y, Z)^\top$ in a space is projected to the point $\boldsymbol{x} = (x, y, z)^\top$ on the hyperbolic surface S according to the formulation

$$\boldsymbol{x} = \lambda \boldsymbol{X}, \tag{6}$$

where

$$\lambda = \frac{\pm a^2}{b\sqrt{X^2+Y^2+Z^2} \mp eZ}. \tag{7}$$

This relation between $\boldsymbol{X}$ and $\boldsymbol{x}$ is satisfied, if the line, which connects the focal point $\boldsymbol{F}$ and the point $\boldsymbol{X}$, and the hyperbolic surface S have at least one real common point. Furthermore, the sign of parameter λ depends on the position of the point $\boldsymbol{X}$ [7]. Hereafter, we assume that the relation of equation (7) is always satisfied. Setting $\boldsymbol{m} = (u, v)^\top$ to be the point on the image plane π, the point $\boldsymbol{x}$ on S is projected to the point $\boldsymbol{m}$ on π according to the equations

$$u = f\frac{x}{z+2e}, \quad v = f\frac{y}{z+2e}, \tag{8}$$

where f is the focal length of the hyperbolic camera. Therefore, a point $\boldsymbol{X} = (X, Y, Z)^\top$ in a space is transformed to the point $\boldsymbol{m}$ as

$$\begin{aligned} u &= \frac{fa^2X}{(a^2 \mp 2e^2)Z \pm 2be\sqrt{X^2+Y^2+Z^2}}, \\ v &= \frac{fa^2Y}{(a^2 \mp 2e^2)Z \pm 2be\sqrt{X^2+Y^2+Z^2}}. \end{aligned} \tag{9}$$

4 Camera-Model Transformation

We present the camera-model transformation from a hyperbolic camera to a panorama camera. Here, setting $\boldsymbol{C}_p$ and $\boldsymbol{F}$ to be the panorama-camera center and the the focal point of the hyperbolic surface S, respectively, we locate $\boldsymbol{C}_p$ and $\boldsymbol{F}$ at the origin of the world coordinate system. Furthermore, for the panorama-camera axis $\boldsymbol{r}_p$ and the hyperbolic-camera axis $\boldsymbol{r}_h$, we set $\boldsymbol{r}_p = \boldsymbol{r}_h = k(0, 0, 1)^\top$ for $k \in \mathbf{R}$, that is, the directions of $\boldsymbol{r}_p$ and $\boldsymbol{r}_h$ are the direction of the z axis. For the configuration of the panorama camera and the hyperbolic camera which share axes $\boldsymbol{r}_p$ and $\boldsymbol{r}_h$ as illustrated in figure 6, the points $\boldsymbol{m} = (u, v)^\top$, $\boldsymbol{x} = (x, y, z)^\top$ and $\boldsymbol{x}_p = (x_p, y_p, z_p)$ are projections of a point $\boldsymbol{X} = (X, Y, Z)^\top$ in a space on to the hyperbolic-image plane π, the the hyperbolic surface S and the cylindrical-image surface S_p, respectively. Here, the points $\boldsymbol{x}$ and $\boldsymbol{m}$ satisfy the equation

$$\boldsymbol{x} = \lambda' \begin{pmatrix} \boldsymbol{m} \\ f \end{pmatrix} + \begin{pmatrix} \boldsymbol{0} \\ -2e \end{pmatrix}, \tag{10}$$

where

$$\lambda' = \frac{a^2}{ef \mp b\sqrt{u^2+v^2+f^2}}. \tag{11}$$

The configuration of the hyperbolic-camera image π and the hyperbolic surface S enables us to set

$$\lambda' = \frac{a^2}{ef - b\sqrt{u^2+v^2+f^2}}. \tag{12}$$

The point $\boldsymbol{x}$ is transformed to the point $\boldsymbol{x}_p$ according to the equation

$$\boldsymbol{x}_p = \frac{f_p}{\lambda' |\boldsymbol{m}|} \boldsymbol{x}. \tag{13}$$

Therefore, equations (10) and (13) derive the relation between the point $\boldsymbol{x}_p$ and $\boldsymbol{m}$ as

$$\boldsymbol{x}_p = \frac{f_p(f - 2e/\lambda')}{|\boldsymbol{m}|} \begin{pmatrix} \frac{\boldsymbol{m}}{f-2e/\lambda'} \\ 1 \end{pmatrix}. \tag{14}$$

These relations permit us to transform the hyperbolic-image plane π to the cylindrical-image surface S_p. This geometrical property leads to the conclusion that a hyperbolic camera and a panorama camera are mathematically equivalent camera models.

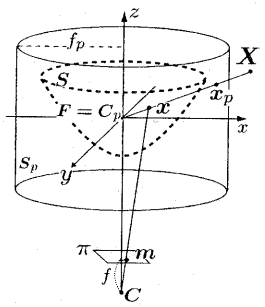

Figure 6: The geometry for the camera transformation from a hyperbolic camera to a panorama camera.

5 Multiple-View Geometry for Panorama Cameras

We consider the imaging region observed by the stereo panorama cameras which are configurated parallel axially, single axially and oblique axially. The parallel-axial and the single-axial stereo cameras image a larger feasible region than the oblique-axial stereo ones. Here, we deal with a camera system of four panorama cameras. The four panorama-camera centers are on the corners of a square vertical to a horizontal plane. Furthermore, all of the camera axes are parallel. Therefore, the panorama-camera centers are $\boldsymbol{C}_a = (t_x, t_y, t_z)^\top$, $\boldsymbol{C}_b = (t_x, t_y, -t_z)^\top$, $\boldsymbol{C}_c = (-t_x, -t_y, t_z)^\top$ and $\boldsymbol{C}_d = (-t_x, -t_y, -t_z)^\top$. This configuration is illustrated in figure 7 (a). Since the epipoles exist on the panorama images and correspond to the camera axes, this camera configuration permits us to eliminate the rotation between the camera coordinate and the world coordinate systems.

For a point $\boldsymbol{X}$, the projections of the point $\boldsymbol{X}$ to cameras $\boldsymbol{C}_a$, $\boldsymbol{C}_b$, $\boldsymbol{C}_c$ and $\boldsymbol{C}_d$ are $\boldsymbol{x}_a = (\cos\theta, \sin\theta, \tan a)^\top$, $\boldsymbol{x}_b = (\cos\theta, \sin\theta, \tan b)^\top$, $\boldsymbol{x}_c = (\cos\omega, \sin\omega, \tan c)^\top$ and $\boldsymbol{x}_d = (\cos\omega, \sin\omega, \tan d)^\top$, respectively, on the cylindrical-image surfaces. These four points are the corresponding-point quadruplet. The points $\boldsymbol{x}_a$, $\boldsymbol{x}_b$, $\boldsymbol{x}_c$ and $\boldsymbol{x}_d$ are transformed to $\boldsymbol{p}_a = (\theta, a)^\top$, $\boldsymbol{p}_b = (\theta, b)^\top$, $\boldsymbol{p}_c = (\omega, c)^\top$ and $\boldsymbol{p}_d = (\omega, d)^\top$, respectively, on the rectangular panoramic images. The corresponding-point quadruplet yields six epipolar planes. Using homogeneous coordinate systems, we represent $\boldsymbol{X}$ as $\boldsymbol{\xi} = (X, Y, Z, 1)^\top$. Here, these six epipolar planes are formulated as

$$\mathbf{M}\boldsymbol{\xi} = 0, \tag{15}$$

where

$$\mathbf{M} = (\boldsymbol{m}_1, \boldsymbol{m}_2, \boldsymbol{m}_3, \boldsymbol{m}_4, \boldsymbol{m}_5, \boldsymbol{m}_6)^\top, \tag{16}$$

$$\boldsymbol{m}_1^\top = \begin{pmatrix} \sin\theta \\ -\cos\theta \\ 0 \\ -\sin\theta t_x + \cos\theta t_y \end{pmatrix}, \tag{17}$$

$$\boldsymbol{m}_2^\top = \begin{pmatrix} \sin\omega \\ -\cos\omega \\ 0 \\ \sin\omega t_x - \cos\omega t_y \end{pmatrix}, \tag{18}$$

$$\boldsymbol{m}_3^\top = \begin{pmatrix} \tan c \sin\theta - \tan a \sin\omega \\ \tan a \cos\omega - \tan c \cos\theta \\ \sin(\omega - \theta) \\ -\sin(\omega - \theta) t_z \end{pmatrix}, \tag{19}$$

$$\boldsymbol{m}_4^\top = \begin{pmatrix} \tan d \sin\theta - \tan b \sin\omega \\ \tan b \cos\omega - \tan d \cos\theta \\ \sin(\omega - \theta) \\ \sin(\omega - \theta) t_z) \end{pmatrix}, \tag{20}$$

$$\boldsymbol{m}_5^\top = \begin{pmatrix} \tan d \sin\theta - \tan a \sin\omega \\ \tan a \cos\omega - \tan d \cos\theta \\ \sin(\omega - \theta) \\ 0 \end{pmatrix}, \tag{21}$$

and

$$\boldsymbol{m}_6^\top = \begin{pmatrix} \tan c \sin\theta - \tan b \sin\omega \\ \tan b \cos\omega - \tan c \cos\theta \\ \sin(\omega - \theta) \\ 0 \end{pmatrix}. \tag{22}$$

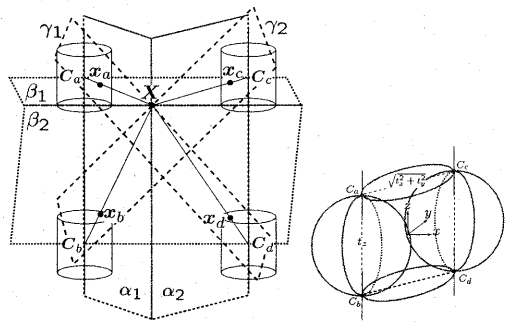

(a) (b)

Figure 7: The configuration of four panorama cameras whose centers are on the corners of a square vertical to a horizontal plane. (a) : The six epipolar planes are yielded by the corresponding-point quadruplet. (b) : The common points of three planes which are orthogonal are determined by the configuration of four panorama cameras.

Since these six planes intersect at the point $\boldsymbol{X}$ in a space, the rank of the matrix $\mathbf{M}$ is three. Therefore, the matrix $\mathbf{M}_R$,

$$\mathbf{M}_R = \begin{pmatrix} m_{i1} & m_{i2} & m_{i3} & m_{i4} \\ m_{j1} & m_{j2} & m_{j3} & m_{j4} \\ m_{k1} & m_{k2} & m_{k3} & m_{k4} \end{pmatrix} = \begin{pmatrix} \boldsymbol{m}_i^\top \\ \boldsymbol{m}_j^\top \\ \boldsymbol{m}_k^\top \end{pmatrix}, \tag{23}$$

is constructed from three row vectors of the matrix $\mathbf{M}$. If and only if the rank of the matrix $\mathbf{M}_R$ is three, $\mathbf{M}_R$ satisfies the equation

$$\mathbf{M}_R \boldsymbol{\xi} = 0. \tag{24}$$

The point $\boldsymbol{X}$ is derived by the equation

$$\boldsymbol{X} = \bar{\mathbf{M}}^{-1} \boldsymbol{m}_4 \tag{25}$$

where

$$\bar{\mathbf{M}} = \begin{pmatrix} m_{i1} & m_{i2} & m_{i3} \\ m_{j1} & m_{j2} & m_{j3} \\ m_{k1} & m_{k2} & m_{k3} \end{pmatrix}, \bar{\boldsymbol{m}}_4 = \begin{pmatrix} -m_{i4} \\ -m_{j4} \\ -m_{k4} \end{pmatrix}. \tag{26}$$

Equation (25) enable us to reconstruct the point $\boldsymbol{X}$ uniquely from any three row vectors selected from the matrix $\mathbf{M}$.

However, the elements of the matrix $\mathbf{M}$ include the numerical errors in their values in the practical use. We evaluate the numerical quantity of the selected row vectors for the reconstruction using the angles between them. Setting

$$g_{\alpha\beta} = \boldsymbol{m}_\alpha^\top \boldsymbol{m}_\beta, \quad \bar{g}_{\alpha\beta} = \bar{\boldsymbol{m}}_\alpha^\top \bar{\boldsymbol{m}}_\beta \tag{27}$$

for $\alpha, \beta = 1, 2, 3$, the matrices

$$\mathbf{G}_R = ((g_{\alpha\beta})), \bar{\mathbf{G}} = ((\bar{g}_{\alpha\beta})) \tag{28}$$

satisfy the relations,

$$\mathbf{G}_R = \mathbf{M}_R \mathbf{M}_R^\top, \quad \bar{\mathbf{G}} = \bar{\mathbf{M}} \bar{\mathbf{M}}^\top. \tag{29}$$

Setting λ_i and σ_i for $i = 1, 2, 3$, to be the eigenvalues of $\mathbf{G}_R$ and $\bar{\mathbf{G}}$, respectively, we can quantitatively evaluate the angles between $\boldsymbol{m}_\alpha$ and $\boldsymbol{m}_\beta$, and $\bar{\boldsymbol{m}}_\alpha$ and $\bar{\boldsymbol{m}}_\beta$, respectively, from the ratios of the eigenvalues. The ratios λ_i/λ_j and σ_i/σ_j determine the approximate dimensions of the volume spanned by the eigenvectors as follows:

1. If the eigenvalues satisfy

$$\lambda_1 \gg \lambda_2 \simeq \lambda_3, \quad \sigma_1 \gg \sigma_2 \simeq \sigma_3, \tag{30}$$

the dimension of the volume spanned by the eigenvectors is approximately one. Therefore, the three row vectors of the matrices $\mathbf{M}_R$ and $\bar{\mathbf{M}}$ are distributed on a line.

2. If the eigenvalues satisfy

$$\lambda_1 \simeq \lambda_2 \gg \lambda_3, \quad \sigma_1 \simeq \sigma_2 \gg \sigma_3, \tag{31}$$

the dimensions of the volume spanned by the eigenvectors are approximately two. Therefore, the three row vectors of the matrices $\mathbf{M}_R$ and $\bar{\mathbf{M}}$ are distributed on a plane.

3. If the eigenvalues satisfy

$$\lambda_1 \simeq \lambda_2 \simeq \lambda_3, \quad \sigma_1 \simeq \sigma_2 \simeq \sigma_3, \tag{32}$$

the dimensions of the volume spanned by the eigenvectors are approximately three. Therefore, the three row vectors of the matrices $\mathbf{M}_R$ and $\bar{\mathbf{M}}$ are distributed in a space.

The point $\boldsymbol{X}$ is derived by the equation (25) as a numerically stable solution if the eigenvalues λ_i and σ_i satisfy the equations (32). Specifically, the conditions

$$\lambda_1 = \lambda_2 = \lambda_3, \quad \sigma_1 = \sigma_2 = \sigma_3, \tag{33}$$

indicate that the three row vectors are mutually orthogonal. These mathematical properties lead to

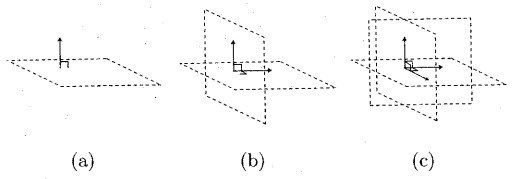

(a) (b) (c)

Figure 8: The approximate dimensions of the eigenvectors are determined by the ratios λ_i/λ_j and σ_i/σ_j. For eqs. (30), (31) and (32), the three row vectors of the matrices $\mathbf{M}_R$ and $\bar{\mathbf{M}}$ are distributed on a line (a), on a plane (b) and in a space (c), respectively.

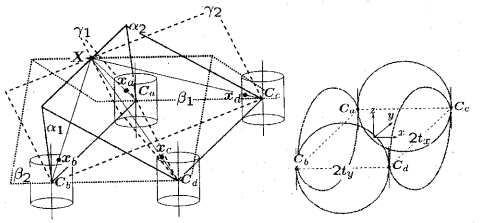

(a) (b)

Figure 9: The configuration of four panorama cameras whose centers are on the corners of a horizontal square. (a) : The six epipolar planes are yielded by the corresponding-point quadruplet. (b) : The common points of three planes which are orthogonal are determined by the configuration of four panorama cameras.

the conclusion that we can select three orthogonal planes from six epipolar planes for the reconstruction of the point $\boldsymbol{X}$. The configuration of four panorama cameras determines the point as the common points of three planes which are orthogonal. The collections of the points are expressed as follows:

1. If $\alpha_1 \perp \alpha_2 \perp \beta_1$

$$X^2 + Y^2 = t_x^2 + t_y^2, \quad Z = t_z. \tag{34}$$

2. If $\alpha_1 \perp \alpha_2 \perp \beta_2$

$$X^2 + Y^2 = t_x^2 + t_y^2, \quad Z = -t_z. \tag{35}$$

3. If $\alpha_1 \perp \beta_1 \perp \beta_2$

$$(X - t_x)^2 + (Y - t_y)^2 + Z^2 = t_z^2. \tag{36}$$

4. If $\alpha_2 \perp \beta_1 \perp \beta_2$

$$(X + t_x)^2 + (Y + t_y)^2 + Z^2 = t_z^2. \tag{37}$$

Equations (34) and (35) geometrically define the circles on a plane in a space. Equations (36) and (37) geometrically define the spheres in a space. Figure 7 (b) shows the two circles and the two spheres defined by equations (34), (35), (36) and (37).

Next, we consider a camera system whose camera centers are configurated on the corners of a horizontal square, and assuming that all of the camera axes are parallel. Here, four panorama-camera centers are $\boldsymbol{C}_a = (t_x, t_y, 0)^\top$, $\boldsymbol{C}_b = (-t_x, t_y, 0)^\top$, $\boldsymbol{C}_c = (-t_x, -t_y, 0)^\top$ and $\boldsymbol{C}_d = (t_x, -t_y, 0)^\top$. This configuration is illustrated in figure 9 (a). The corresponding-point quadruplet for a point in a space yields six epipolar planes. The three planes selected from the four epipolar planes intersect orthogonally on a common point. The collections of the common points of three planes which are orthogonal are expressed as follows:

1. If $\alpha_1 \perp \alpha_2 \perp \beta_1$

$$X^2 + Z^2 = t_x^2, \quad Y = t_y. \tag{38}$$

2. If $\alpha_1 \perp \alpha_2 \perp \beta_2$

$$Y^2 + Z^2 = t_y^2, \quad X = -t_x. \tag{39}$$

3. If $\alpha_1 \perp \beta_1 \perp \beta_2$

$$X^2 + Z^2 = t_x^2, \quad Y = -t_y. \tag{40}$$

4. If $\alpha_2 \perp \beta_1 \perp \beta_2$

$$Y^2 + Z^2 = t_y^2, \quad X = t_x. \tag{41}$$

Equations (38), (39), (40) and (41) geometrically define the circles on a plane in a space. Figure 9 (b) shows the circles defined by these equations.

For the configurations of cameras in figure 7 (a) and figure 9 (a), the four panorama-camera centers are located on a vertical plane and a horizontal plane, respectively, in a space. If a point in a space are on this plane, all elements of a corresponding-point quadruplet for the point are mutually coplanar on this plane. The six epipolar planes yielded

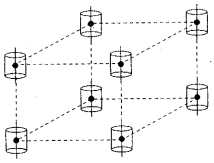

Figure 10: The configuration for eight panorama cameras.

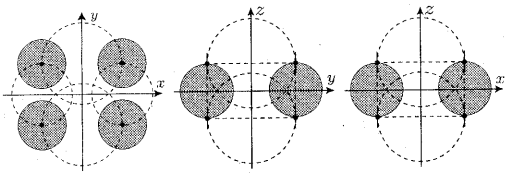

(a) (b) (c)

Figure 11: The gray circles in figures are the spheres. The dashed lines in these figures are the circles on a plane in a space. These spheres and circles are yielded by the collections of common points of three orthogonal planes selected from 28 epipolar planes.

by a corresponding-point quadruplet for the point coinside to a plane. Therefore, the point on this plane is not possible to reconstruct from the geometrical constraint of the six epipolar planes.

Finally, we propose a camera system with eight panorama cameras combinating the two configurations of four panorama cameras shown in figure 7 (a) and figure 9 (a). Therefore, the eight panorama-camera centers are on the corners of a parallel pipe. This configuration is illustrated in figure 10. The corresponding-point octuplet for a point in a space yields 28 epipolar planes. Same as the four panorama-camera system, this eight panorama-camera system enables us to select three orthogonal planes, which orthogonally intersect on a common point, from the 28 epipolar planes. The collections of common points of three epipolar planes yield the 16 circles and the 8 spheres as illustrated in figure 11.

Since cameras of this system are configurated in a space, this camera system can yield more combinations of orthogonal planes than the four camera system dose. Therefore, the points which are the common points of these orthogonal planes distribute in wider areas in a space. Furthermore, because of the combination of the two planar configurations, the configuration in a space of eight cameras has no critical point which are not reconstructed. This geometrical property leads to the conclusion that our eight panorama-camera system provides a larger feasible region for the reconstruction of objects than four-camera system on a plane.

6 Summary and Conclusions

In this paper, we formulated quadrilinear forms for the multiple images observed by panorama and omni-directional cameras. We observed that multiple-focal-tensorial expression is a natural mathematical tool for the analysis of multiple panorama-camera system.

References

[1] Faugeras, O.: *Three-Dimensional Computer Vision, A Geometric Viewpoint.* MIT Press, Cambridge, MA, 1993.

[2] Hartley, R., Zisserman, A.: Trifocal tensor, In *Multiple View Geometry in Computer Vision.* chap. 14, pp. 355–378, Cambridge University Press, Cambridge, 2000.

[3] Shashua, A.: Trilinear tensor: The fundamental construct of multiple-view geometry and its applications. *International Workshop on Algebraic Frames For The Perception Action Cycle*, Kiel Germany, 1997.

[4] Shashua, A., Wolf, L.: On the structure and properties of the quadrifocal tensor. *ECCV*, June 2000, Dublin, Ireland.

[5] Hartley, R. I.: Computation of the quadrifocal tensor. *ECCV-A* 98, 1998, pp. 20–35.

[6] Kanade, T., Morris, D. D.: Factorization methods for structure from motion, *Philosophical Transactions of the Royal Society*, Series A, Vol. 356, No. 1740, pp. 1153–1173.

[7] Svoboda, T., Pajdla, T., Hlavac, V.: Epipolar geometry of panoramic cameras. *ECCV-A* 98, 1998, pp. 218–231.

[8] Sugimura, T., Sato, J.: Robust computation of trifocal tensor from mutual projection of cameras. *Meeting on Image Recognition and Understanding*, Vol. II, Nagoya, 2002, pp. 239–246.

[9] Daniilidis, K., Geyer, C.: Omnidirectional vision: theory and algorithms. *ICPR01* Vol. I. pp. 89–96.